International Journal of Modern Physics B
Vol. 31 (2017) 1750244 (33 pages)

DOI: 10.1142/S0217979217502447

Approach to equilibrium of a quantum system and generalization of the Montroll–Shuler equation for vibrational relaxation of a molecular oscillator

V. M. Kenkre* and M. Chase†

Consortium of the Americas for Interdisciplinary Science, University of New Mexico, Albuquerque, NM 87131, USA

Department of Physics and Astronomy, University of New Mexico, Albuquerque, NM 87131, USA
**kenkre@unm.edu*
†mchase@unm.edu

Received 25 May 2017
Accepted 6 June 2017
Published 22 June 2017

The approach to equilibrium of a quantum mechanical system in interaction with a bath is studied from a practical as well as a conceptual point of view. Explicit memory functions are derived for given models of bath couplings. If the system is a harmonic oscillator representing a molecule in interaction with a reservoir, the generalized master equation derived becomes an extension into the coherent domain of the well-known Montroll–Shuler equation for vibrational relaxation and unimolecular dissociation. A generalization of the Bethe–Teller result regarding energy relaxation is found for short times. The theory has obvious applications to relaxation dynamics at ultra-short times as in observations on the femtosecond time scale and to the investigation of quantum coherence at those short times. While vibrational relaxation in chemical physics is a primary target of the study, another system of interest in condensed matter physics, an electron or hole in a lattice subjected to a strong DC electric field that gives rise to well-known Wannier–Stark ladders, is naturally addressed with the theory. Specific system–bath interactions are explored to obtain explicit details of the dynamics. General phenomenological descriptions of the reservoir are considered rather than specific microscopic realizations.

Keywords: Approach to equilibrium; Montroll-Shuler equation; vibrational relaxation.

PACS numbers: 05.30.-d, 05.60.Gg

*Corresponding author.

1. Introduction

Investigations into the time evolution of the process of relaxation of a quantum mechanical system in interaction with a bath draw their importance from practical as well as conceptual sources. Situations are often met within which the quantum mechanical system is prepared in some particular state and allowed to return to its equilibrium configuration as a consequence of its interaction with the bath. A common example is encountered when light made to shine on a material raises a molecule to an excited state, and its relaxation back into normal equilibrium needs to be described and manipulated.[1–16] An understanding of the process of relaxation into equilibrium can be of interest in a variety of processes including unimolecular dissociation[17] and other chemical reactions,[18] gentle or explosive.[19,20] The conceptual importance should be obvious. Knowing how an arbitrary system disturbed from equilibrium returns to the equilibrium state described by the postulates of equilibrium statistical mechanics is an aim important in its own right as details of the process whereby Boltzmann weights are achieved among the probabilities of occupation of the systems and, simultaneously, decoherence leads to the randomization of phases[21–24] are not fully understood. Our study has as its aims both these aspects, conceptual understanding of the basic tenet of statistical mechanics and practical insight into the relaxation of specific quantum systems.[25–27] The latter, along with a detailed theoretical understanding of quantum mechanical evolution at very short times, has become important since the proliferation of femtoscale experiments and the advent of even faster spectroscopy.[18,25–29]

Consider an isolated system with Hamiltonian H and therefore a spectrum of energies corresponding to the various eigenstates of H. If we put the system initially in one of those eigenstates, nothing will obviously happen, in the sense that the system will stay in that state, the phase merely evolving periodically in time. When we encounter the system without any given preparation into a specific state, we always invoke the postulate of equilibrium statistical mechanics (see any common text such as by Huang[21]), that the system density matrix will be diagonal in the representation of the eigenstates and that its diagonal elements will have Boltzmann weights in that representation. We wish to draw attention here to the split nature of the postulate, made particularly clear by the text mentioned: one part referring to the probabilities and the other to the phases. Invoking the postulate means that we tacitly (and naturally) assume that the system is not really isolated but that there is an interaction of the system with the rest of the universe, or, simply put, with a bath. The system–bath interaction must have certain properties for the postulate to be valid. The interaction must be *strong* enough, and of such a nature, that, whatever the initial state, the evolution will drive the system to a state with random phases and Boltzmann weights characteristic of the temperature of the bath. Yet the interaction must be *weak* enough so that, in the representation of the eigenstates of the given isolated system, the state reached at equilibrium is diagonal and Boltzmann-weighted, *no vestige* of the bath, other

than the value of the temperature, being left in the state that the system arrives at. Maintaining this weak-interaction qualification, let us ask for an evolution equation which can describe the approach to equilibrium accurately, *including at times short* with respect to the equilibration. This is the purpose of the present paper.

If the interest is simply in the final (equilibrium) state, there is little to study since we know it already as given by the split postulate of equilibrium statistical mechanics (Boltzmann weights and random phases both in the H eigenstates representation). If the interest is in the long-time evolution to the equilibrium state, the answer is also known as given by a master equation for the probabilities of occupation of the H eigenstates with detailed balance operating between the transition rates. Typically, the off-diagonal elements of the density matrix are considered irrelevant at the level of such a coarse description. Although a number of theoretical approaches have been developed more recently,[2–4,10–12,16,30] the master equation that has been a workhorse in chemical physics for the study of vibrational relaxation for almost 70 years is the Montroll–Shuler (MS) equation.[9] Many details of the properties of the Montroll–Shuler equation, the system evolution it describes and extensions for various purposes have been worked out in the literature. See, for example, Refs. 14, 15 and 31–33.

However, what is not known well is the evolution equation we should write down if our interest is also in the short time evolution. As a result of the fundamental researches carried out by a number of theorists[34–43] including, in particular, Zwanzig,[35–38] it is known that a formalistic answer capable of continuously linking the short-time evolution to its long-time evolution counterpart is available in principle. The relevant equation is the forced generalized master equation (GME) obeyed by the probabilities of the Hamiltonian eigenstates; the forcing term is determined by the initial condition of the system. The nature of the bath influences both this forcing term and the memory functions. Required is an explicit and usable equation, not merely an abstract formalism. This is by no means a trivial issue because the bath must be minimalistic in that it must drive the system to a density matrix, which, in its own H-eigenstate representation, is diagonal and Boltzmann-weighted in the system, *without leaving any other signatures* of the nature of the bath in the final state. Below we make an attempt to provide such a useable equation in the form of an extension of the Montroll–Shuler equation.

For simplicity, we will begin assuming in the tradition of van Hove,[34] Zwanzig[35–38] and others[39–43] that there is no forcing term in the equation and that this is ensured, in the standard manner, by an initial random phase condition. The absence of the initial condition term will be always valid if the system is initially in a *single* eigenstate of H. We will return to the effect[44] of nonvanishing initial condition forcing terms in a subsequent publication. In the absence of those terms, the probabilities of occupation P of the system among its H-eigenstates, which we will denote by M, N, etc., obey, as known from the traditional

literature,[35–40,44,45]

$$\frac{dP_M(t)}{dt} = \int_0^t dt' \sum_N \left[\mathcal{W}_{MN}(t-t')P_N(t') - \mathcal{W}_{NM}(t-t')P_M(t')\right]. \tag{1}$$

The precise manner in which the approach to equilibrium will proceed in time will indeed depend on the nature of bath even though the final state will not. We will see in Appendix A that, under the simplification that the bath effects can be characterized by a single[45] bath function $Y(z)$, the memory functions $\mathcal{W}(t)$ are given by Fourier-transform expressions

$$\int_{-\infty}^{\infty} dz Y(z) \cos\left[(z \pm \Delta E)t\right],$$

the system energy difference between the states considered being denoted by ΔE. The $\pm$ refers to the two directions of transitions (energetically downward or upward). The long-time *rates* bear detailed balance ratios to each other and thereby ensure Boltzmann weights of the system probabilities in the steady state. The memory functions $\mathcal{W}(t)$ do not bear such ratios for all times but their time integrals (from 0 to ∞), which *are precisely* the transition rates between the two states, do. Indeed, if the bath is truly deserving of the name, it would bring any system put in interaction with it to the same temperature T characteristic of itself. For this purpose, $Y(z)$ needs to satisfy a special condition which is

$$Y(-z) = Y(z)e^{-\beta z}, \tag{2}$$

where $\beta = 1/k_B T$, k_B being the Boltzmann constant and T the bath temperature. An alternative form of this condition is

$$Y(z) = \frac{Y_s(z)}{1 + e^{-\beta z}}, \tag{3}$$

where $Y_s(z) = Y_s(-z)$ is symmetric in z. Various baths will differ in the actual form of $Y_s(z)$ but will all produce the required approach to equilibrium of the system at the bath temperature T as a result of Eq. (3), which ensures the property in Eq. (2).

The present paper is laid out as follows. The necessary formalism to arrive at the above evolution equations is given, only in essentials, in Appendix A. The effects of the memory functions thereby obtained are explored in Secs. 2 and 3 for two systems. The first is our primary target of study, viz., an excited molecule undergoing vibrational relaxation. The second is a related condensed matter system we report on, a charged particle in a crystal accelerated by the strong electric fields leading to the formation of Wannier–Stark ladders. In Sec. 2, the GME that naturally extends the Montroll–Shuler equation[9] into the coherent domain is developed and explored. The evolution of the Montroll–Shuler generating function thus generalized under coherence conditions is examined. An explicit solution is obtained in the Laplace domain for initial Boltzmann conditions at a temperature different from that of the bath and a query is made into the so-called canonical evolution.[32,33]

Moments are calculated and a result obtained previously by Bethe and Teller[46] for long times for the evolution of the average energy of the relaxing molecule is generalized for short times during which decoherence occurs. These should have relevance to time-resolved ultrafast observations made by Zewail and collaborators.[18,25–27] In Sec. 3, where motion of a charge on a lattice under strong electric fields is analyzed to illustrate the dynamics of a related system, the GME obtained under the weak-coupling approximation with the bath is solved and expressions for the propagator in the Laplace domain are given. The time-domain dynamics of the charge are discussed and comparisons made with the short-time coherent evolution and long-time dynamics. Illustrative, but explicit, analytic bath function calculations are presented in Sec. 4 without assuming microscopic details of the bath such as whether it consists of harmonic oscillators, free colliding particles, two-state systems, etc. Microscopic underpinnings for the bath memories will be derived and discussed in a subsequent article under preparation. Section 5 presents conclusions.

2. Beyond the Montroll–Shuler Equation for Vibrational Relaxation of a Molecule

The equation introduced into the theory of vibrational relaxation by Shuler with his collaborators[7–9] and solved completely in its general, discrete, form by Montroll and Shuler[9] is given by

$$\frac{dP_M}{dt} = \kappa[(M+1)P_{M+1} + Me^{-\beta\Omega}P_{M-1} - (M + (M+1)e^{-\beta\Omega})P_M]. \qquad (4)$$

Here $P_M(t)$ is the probability that the oscillator can be found in the Mth energy level of the harmonic oscillator, Ω is the difference in energy between levels, equivalently the frequency of the oscillator since we have put $\hbar = 1$ throughout this paper, κ is the relaxation rate and $\beta = 1/k_BT$ as mentioned above. All frequencies are given in units of κ. The well-known basis of the master equation (4) is Landau–Teller transitions[47] that arise from an interaction of the harmonic oscillator with the bath, taken to be linear in the oscillator coordinate.

On the basis of the Zwanzig procedure of diagonalizing projection operators[35–38] generalized via coarse-graining as given by one of the present authors,[45,48,49] we write the GME for vibrational relaxation following the methodology sketched in Appendix A. The GME is capable of describing the combined process of decoherence and population for conditions in which the oscillator density matrix is initially diagonal in its Hamiltonian eigenstates. In order to understand the formal connection of our GME to the Montroll–Shuler equation (4), let us first observe that the latter has $(M+1)P_{M+1} - MP_M$ as the terms describing energetically upward transitions and $e^{-\beta\Omega}[MP_{M-1} - (M+1)P_M]$ as those describing downward transitions; the detailed balance factor $e^{-\beta\Omega}$ makes the difference particularly transparent. Let us, accordingly, rearrange the terms in Eq. (4):

$$\frac{1}{\kappa}\frac{dP_M}{dt} = [(M+1)P_{M+1} - MP_M] - e^{-\beta\Omega}[(M+1)P_M - MP_{M-1}]. \qquad (5)$$

The calculations in Appendix A indicate that the generalization for the description of decoherence results simply in the respective terms being multiplied by memories $\phi_-(t)$ and $\phi_+(t)$, respectively. The generalization we present is, thus, the GME

$$\frac{1}{\kappa}\frac{dP_M(t)}{dt} = \int_0^t dt'\phi_-(t-t')[(M+1)P_{M+1}(t') - MP_M(t')] - \phi_+(t-t')[(M+1)P_M(t') - MP_{M-1}(t')]. \quad (6)$$

The memory functions $\phi_\pm(t)$ do not bear to each other a detailed balance ratio at every t but their time integrals, as t goes from 0 to ∞, do. Typically, the memories are rapidly decaying functions and the Markoffian approximation.

$$\phi_-(t) \approx \delta(t)\left[\int_0^\infty dt'\phi_-(t')\right], \quad \phi_+(t) \approx \delta(t)e^{-\beta\Omega}\left[\int_0^\infty dt'\phi_-(t')\right],$$

allows the Montroll–Shuler equation to be recovered from our GME, see Eq. (6). For times short with respect to the decay time of the memories, Eq. (6) describes coherent phenomena such as oscillations not present in predictions of Eq. (5).

We have focused only on the probability evolution. The effects of the evolution of the off-diagonal elements of the oscillator density matrix are by no means neglected, however. Taking them, as well as the reservoir dynamics, into account leads to the introduction of the ingredient in Eq. (6) that makes it an *extension* of the Montroll–Shuler equation[9] capable of describing quantum mechanical decoherence. This ingredient is the memory function pair $\phi_\pm(t)$.

The memory functions arise from the interactions of the bath with the relaxing molecule (modeled here as a harmonic oscillator of frequency Ω). The calculation is outlined in Appendix A and the consequences of the specific features of the bath spectral function on the time dependence of the memories are elaborated on in Sec. 4 below. Our explicit calculations use the general, physically transparent, Fourier-transform prescription first presented in Ref. 45 which expresses the memories in terms of the spectral function $Y(z)$ of the bath:

$$\kappa\phi_\pm(t) = \int_{-\infty}^{\infty} dz Y(z)\cos((z \pm \Omega)t). \quad (7)$$

The Markoffian approximation of this equation makes clear the relation,

$$\kappa = \pi Y(\Omega) = \pi Y(-\Omega)e^{\beta\Omega},$$

of the relaxation rate κ and the bath spectral function, as well as the thermal property of the bath spectral function required by detailed balance and given in Eq. (2). We see that we may define, for later use, a sum-memory $\phi_S(t)$ as

$$\kappa\phi_S(t) = \kappa[\phi_-(t) + \phi_+(t)], \quad (8)$$

which is the product of $2\cos\Omega t$ and the cosine transform of $Y(z)$, and a difference-memory $\phi_\Delta(t)$ as

$$\kappa\phi_\Delta(t) = \kappa[\phi_-(t) - \phi_+(t)], \quad (9)$$

which is the product of $2\sin\Omega t$ and the sine transform of $Y(z)$.

The explicit generalization (6) of the Montroll–Shuler equation (4) or (5) is one of the new results in this paper. With its help we have

- obtained an explicit extension to the coherent domain of the generating function evolution given in Ref. 9;
- obtained equations for arbitrary-order moments and factorial moments of the probability distribution;
- investigated the Bethe–Teller prediction[46] of the independence of the time evolution of the average energy of the relaxing oscillator on the particulars of the initial probability distribution, and
- investigated the property of canonical invariance[32,33] through an explicit solution of the generating function equation in the Laplace domain.

We describe these four results below.

2.1. *First-order partial differential equation for the generating function*

The analysis of Montroll and Shuler[9] owes its success to the introduction of a powerful technique which is based on the transformation of the probabilities into the generating function

$$G(z,t) = \sum_{M=0}^{\infty} z^M P_M(t). \tag{10}$$

We maintain the Montroll–Shuler notation that the generating function argument is z. No confusion should occur with the use of the same variable for describing frequency of the bath spectral function $Y(z)$ for instance in Sec. 4. The transformation converts Eq. (5) into

$$\frac{1}{\kappa}\frac{\partial G(z,t)}{\partial t} = (z-1)\frac{\partial}{\partial z}[(ze^{-\theta}-1)G(z,t)], \tag{11}$$

where $\theta = \Omega/k_BT$ is the ratio of the system energy to the thermal energy of the bath. It is clear that the transformation [Eq. (10)] when applied to our GME, Eq. (6), predicts a simple generalization of Eq. (11) valid for arbitrary coherence,

$$\frac{1}{\kappa}\frac{\partial G(z,t)}{\partial t} = (z-1)\frac{\partial}{\partial z}\int_0^t dt'[(z\phi_+(t-t') - \phi_-(t-t'))G(z,t')]. \tag{12}$$

The power of the Montroll–Shuler analysis comes from the solution of Eq. (11), a first-order partial differential equation for the generating function, by the method of characteristics. All that is necessary to obtain the exact solution $G(z,t)$ of Eq. (11) for *any* initial condition is to calculate the initial value of $G(z,t)$:

$$G(z,0) = \sum_{M=0} z^M P_M(0) = G_0(z).$$

The exact solution for all t would then be obtained as

$$G(z,t) = \frac{1-e^{-\theta}}{(z-1)e^{-\tau}e^{-\theta} - (ze^{-\theta}-1)} G_0[\zeta(z)]. \tag{13}$$

Here, $\tau \equiv \kappa t(1-e^{-\theta})$ and the second factor in Eq. (13) is simply $G_0(z)$ with z substituted by the function $\zeta(z)$ given by

$$\zeta(z) = \frac{(z-1)e^{-\tau} - (ze^{-\theta}-1)}{(z-1)e^{-\tau}e^{-\theta} - (ze^{-\theta}-1)}. \tag{14}$$

This remarkable recipe provided by Montroll and Shuler allows one to obtain, through an inverse transformation, the probabilities $P_M(t)$ for all times.

While we have not been able to similarly solve the integro-differential equation, Eq. (12), for arbitrary initial conditions, we have obtained several partial results.

2.2. *Moment and factorial moment equations from the GME*

Using the factorial moment

$$f_M(t) = \sum_N N(N-1)\cdots(N-M+1)P_N(t), \tag{15}$$

Montroll and Shuler obtained the simple equation

$$\frac{1}{\kappa}\frac{df_M}{dt} + M(1-e^{-\theta})f_M = M^2 e^{-\theta} f_{M-1}. \tag{16}$$

Our generalization from the GME turns out to be also simple:

$$\frac{1}{\kappa}\frac{\partial f_M(t)}{\partial t} + M\int_0^t dt' \phi_\Delta(t-t') f_M(t') = M^2 \int_0^t dt' \phi_+(t-t') f_{M-1}(t'). \tag{17}$$

Here we see the natural appearance of the difference-memory function $\phi_\Delta(t)$ defined in Eq. (8) and note that its time integral from 0 to ∞ equals $1-e^{-\theta}$. The evolution equations for the direct moments have a slightly more complicated form:

$$\frac{1}{\kappa}\frac{d\langle M^n\rangle}{dt} + n\phi_\Delta * \langle M^n\rangle = \sum_{p=1}^{n-1} \binom{n}{p-1} \left[\frac{(n+1)}{p}\phi_+ - (-1)^{n-p}\phi_-\right] * \langle M^p\rangle + \phi_+ * 1, \tag{18}$$

where we use the notation $g * f = \int_0^t dt' g(t-t') f(t')$. The first and second moments obey

$$\frac{1}{\kappa}\frac{d\langle M\rangle}{dt} + \int_0^t dt' \phi_\Delta(t-t')\langle M\rangle(t') = \int_0^t dt' \phi_+(t'), \tag{19a}$$

$$\frac{1}{\kappa}\frac{d\langle M^2\rangle}{dt} + 2\int_0^t dt' \phi_\Delta(t-t')\langle M^2\rangle(t') = \int_0^t dt' [\phi_\Delta(t-t') + 4\phi_+(t-t')]\langle M\rangle(t') + \int_0^t dt' \phi_+(t'). \tag{19b}$$

It is thus seen that the memory combinations that occur are $\phi_\Delta(t)$ and $\phi_+(t)$. Their form for the various baths can be gleaned in Sec. 4; under the Markoffian approximation they are the products of $\delta(t)$ and, respectively, $1-e^{-\theta}$ and $e^{-\theta}$. We remind the reader that as in the analysis of Montroll and Shuler we use the symbol $\theta = \beta\Omega$.

2.3. *Study of the validity of the Bethe–Teller result in the coherent domain*

In an important investigation of deviations from thermal equilibrium in shock waves,[46] Bethe and Teller found that the average energy $E(t)$ of a molecule in a reservoir would relax exponentially from its initial value $E(0)$ to the thermal value $E_{\rm th} = (\Omega/2)\coth(\theta/2)$ according to

$$E(t) = E(0)e^{-\kappa(1-e^{-\theta})t} + E_{\rm th}(1 - e^{-\kappa(1-e^{-\theta})t}). \tag{20}$$

This result can also be seen in the later work of Rubin and Shuler[7] and of Montroll and Shuler.[9] There are two important questions here. The first is whether the time dependence of the relaxation of the energy is different for different initial values of the energy; the second is whether it depends on the particular form of the initial distribution of the energy among the energy levels of the molecule for a given value of the initial energy. The answers in the work of Bethe and Teller, which are the same as those emerging from the Montroll–Shuler equation, are that the time dependence is exponential throughout the evolution and that this exponential nature is independent of the initial details of the distribution. The latter result is in contrast to the evolution of the probabilities themselves which do depend on their initial values.

In the context of our present investigation which addresses an arbitrary degree of coherence in the vibrational relaxation, we also find, as in the Bethe–Teller analysis, that the initial details of the probability distribution do not influence the time dependence of the average energy; and that the initial value of the average energy does so only in a trivial (multiplicative) way. However, we do expect that if the time evolution shows an exponential nature, it would do so only in the long-time limit when the Markoffian approximation becomes valid. We study now the departures that occur at short times.

The answers in the presence of coherence are in the moment equations that we have derived above. Below, and henceforth throughout the paper, ϵ is the Laplace variable and tildes denote Laplace transforms. We find in the Laplace domain our new result for the dynamics of the energy valid for an arbitrary degree of coherence:

$$\widetilde{E}(\epsilon) = \frac{E(0)}{\epsilon + \kappa\widetilde{\phi}_\Delta(\epsilon)} + E_{\rm th}\left[\frac{\widetilde{\phi}_S(\epsilon)}{\widetilde{\phi}_\Delta(\epsilon)}\tanh\left(\frac{\theta}{2}\right)\right]\left[\frac{1}{\epsilon} - \frac{1}{\epsilon + \kappa\widetilde{\phi}_\Delta(\epsilon)}\right]. \tag{21}$$

The Markoffian limit of the energy relaxation dynamics we have obtained yields the Bethe–Teller or Montroll–Shuler result in an interesting way. Abelian theorems

can be invoked to obtain the time-domain limiting values at large times of the memories $\phi(t)$ as the limiting values of $\epsilon\widetilde{\phi}(\epsilon)$ as ϵ tends to zero. We recall that the ratio of the time integrals from 0 to ∞ of the sum- and difference-memories, $\phi_S(t)$, $\phi_\Delta(t)$, equals $\coth(\theta/2)$. This renders the contents of the first square bracket in Eq. (21) equal to 1 as ϵ tends to zero. If we write

$$\widetilde{\eta}(\epsilon) = \frac{1}{\epsilon + \kappa\widetilde{\phi}_\Delta(\epsilon)},$$

in other words denote the first term on the right-hand side of Eq. (21) as the Laplace transform of $E(0)\eta(t)$, we see that the last square bracket in Eq. (21) is the Laplace transform of $1-\eta(t)$. Thus, the generalization of Eq. (20) that arises from our GME analysis,

$$E(t) = E(0)\eta(t) + E_{\rm th}\int_0^t dt'\xi(t-t')[1-\eta(t')], \tag{22}$$

maintains a form that is almost identical to the Bethe–Teller evolution. The only differences are the nonexponential nature of $\eta(t)$ in the presence of coherence and the existence of the convolution with $\xi(t)$, a function that is defined through its Laplace transform via

$$\widetilde{\xi}(\epsilon) = \frac{\widetilde{\phi}_S(\epsilon)}{\widetilde{\phi}_\Delta(\epsilon)}\tanh\left(\frac{\theta}{2}\right).$$

We display in Fig. 1 the oscillatory relaxation of the energy for coherent conditions. The Lorentzian bath memory is taken for different assumed spectral widths and the resulting oscillations in the relaxation, our generalization of the Bethe–Teller result, are shown along with the incoherent limit. See figure caption. The memories are responsible for the coherent behavior at short times but at long times reproduce the Montroll–Shuler or Bethe–Teller behavior. As explained above, this happens because in the Markoffian limit $\eta(t)$ becomes $e^{-\kappa(1-e^{-\theta})t}$, and the ratio of the time integrals from 0 to ∞ of the sum- and difference-memories, $\int_0^\infty dt\phi_S(t)/\int_0^\infty dt\phi_\Delta(t)$, exactly equals $\coth(\theta/2)$.

2.4. *Lack of canonical invariance of the GME*

The general solution for the generating function for the MS equation, Eq. (13), is simplified a great deal when the initial distribution is taken to have Boltzmann weights among the states corresponding to an "initial" temperature T_0. With the notation $\theta_0 = \Omega/k_BT_0$, the initial value of the generating function is given by

$$G_0(z) = \frac{1-e^{-\theta_0}}{1-ze^{-\theta_0}}.$$

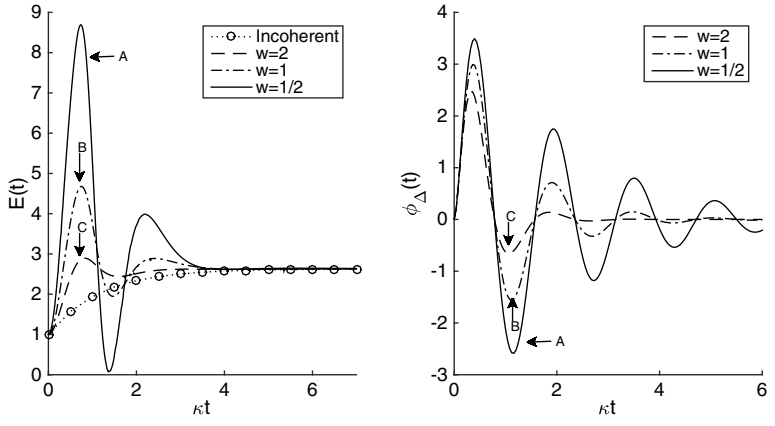

Fig. 1. Generalization of the Bethe–Teller result for coherent conditions. Shown in the left panel is the time evolution of the average energy of the relaxing molecule, $E(t)$, normalized to its initial value $E(0)$, as a function of the dimensionless time κt. The energy rises from its initial value and saturates to the thermal value $E_{\rm th}$ [see Eq. (22)], the incoherent limit given by the Bethe–Teller result, Eq. (20). This incoherent result is a simple exponential rise and is labeled by the symbol o. Coherent cases of the bath spectral function, assumed Lorentzian as in Eq. (37), with respective (illustrative) scaled values of w as 2, 1, and 1/2 lead to oscillations in the energy with larger and larger amplitudes of oscillation. The three difference-memory functions $\phi_\Delta(t)$ from Eq. (38), corresponding to the three examples of the nonmonotonic evolution of the average energy, are shown in the right panel. Assumed scaled values of other parameters, temperature and molecular frequency, are illustrative, $\beta = 1/2$ and $\Omega = 4$.

Upon the replacement of the argument of G_0 with $\zeta(z)$, and subsequent expansion of Eq. (13), the solution to the generating function simplifies into

$$G(z,t) = \left[\frac{\widetilde{\phi}_+(0) - \widetilde{\phi}_-(0)}{z\widetilde{\phi}_+(0) - \widetilde{\phi}_-(0)}\right]\left[\frac{1}{1 - \frac{(z-1)(\widetilde{\phi}_+(0) - e^{-\theta_0}\widetilde{\phi}_-(0))}{(z\widetilde{\phi}_+(0) - \widetilde{\phi}_-(0))(1-e^{-\theta_0})}e^{-\tau}}\right], \tag{23}$$

where we highlight the connection to the GME by replacing at the appropriate places 1 and $e^{-\theta}$ with the respective time integrals $\widetilde{\phi}_\mp(\epsilon = 0)$ relevant to the Markoffian approximation.

Notice that the right-hand side of Eq. (23) is of the form $C/(1-Ae^{-Bt})$, where A, B and C are all constants. The Laplace transform is trivially written by expanding the fraction in a power series. The Laplace transform of Eq. (23) is

$$\widetilde{G}(z,\epsilon) = \left[\frac{\widetilde{\phi}_+(0) - \widetilde{\phi}_-(0)}{z\widetilde{\phi}_+(0) - \widetilde{\phi}_-(0)}\right]\sum_k \frac{\frac{1}{\kappa}}{\frac{\epsilon}{\kappa} + k(\widetilde{\phi}_-(0) - \widetilde{\phi}_+(0))}$$
$$\times \left[\frac{(z-1)(\widetilde{\phi}_+(0) - e^{-\theta_0}\widetilde{\phi}_-(0))}{(z\widetilde{\phi}_+(0) - \widetilde{\phi}_-(0))(1-e^{-\theta_0})}\right]^k, \tag{24}$$

where the k-summation is over integers from 0 to ∞. Equation (24) is the solution to the first-order differential equation with respect to z for the generating

function, i.e.,

$$(z-1)\left[\frac{\partial}{\partial z}[z\widetilde{\phi}_+(0)\widetilde{G}(z,\epsilon)] - \frac{\partial}{\partial z}\widetilde{\phi}_-(0)\widetilde{G}(z,\epsilon)\right] = \frac{\epsilon}{\kappa}\widetilde{G}(z,\epsilon) - \frac{1}{\kappa}\frac{1-e^{-\theta_0}}{1-ze^{-\theta_0}},$$

when ϵ in $\widetilde{\phi}_\pm(\epsilon)$ is set to zero. In the presence of coherence, we have to find the solution of an equation that is identical to the above except for the replacement of $\epsilon = 0$ memories by ϵ-dependent counterparts. Noticing that the procedure for the solution of the partial differential equation in z has nothing to do with the ϵ-dependence of the memories, we obtain the full solution in the Laplace domain when ϵ in $\widetilde{\phi}_\pm$ is arbitrary as

$$\widetilde{G}(z,\epsilon) = \left[\frac{\widetilde{\phi}_+(\epsilon)-\widetilde{\phi}_-(\epsilon)}{z\widetilde{\phi}_+(\epsilon)-\widetilde{\phi}_-(\epsilon)}\right]\sum_k \frac{\frac{1}{\kappa}}{\frac{\epsilon}{\kappa}+k(\widetilde{\phi}_-(\epsilon)-\widetilde{\phi}_+(\epsilon))} \times\left[\frac{(z-1)(\widetilde{\phi}_+(\epsilon)-e^{-\theta_0}\widetilde{\phi}_-(\epsilon))}{(z\widetilde{\phi}_+(\epsilon)-\widetilde{\phi}_-(\epsilon))(1-e^{-\theta_0})}\right]^k. \quad (25)$$

To ensure that this nonstandard manner of obtaining the solution that we give is indeed accurate, it is necessary to substitute the suggested expression (25) in the Laplace transform of Eq. (12). We have carried this out and shown explicitly that the solution is indeed accurate.

For canonical invariance to hold, the time-domain generating function must be of the form

$$G(z,t) = \frac{1-e^{-\Theta(t)}}{1-ze^{-\Theta(t)}},$$

where $\Theta(t)$ gives the time dependence of the temperature. A direct inversion of Eq. (25) is analytically intractable for arbitrary bath memories ϕ. However, one can easily see, from considerations of Eq. (25), that $G(z,t)$ involves multiple temporal convolutions for a general memory. Thus, no $\Theta(t)$ exists. Canonical invariance of the solution only sets in at sufficiently long times when it is assured by the same arguments that hold in the original analysis for the incoherent master equation.[32,33]

3. Quantum Evolution in a Related System: Stark Ladders in a Crystal

A pedagogically simple quantum system to consider, in discussing the nuances of the combined decoherence and population relaxation processes during the approach to equilibrium, is a nonresonant dimer which has two nondegenerate states.[50] The molecule relaxing vibrationally in interaction with a reservoir discussed in the previous section can be considered to be a realistic extension of that nonresonant dimer. The extension introduces complications, consequently richness of behavior, that arise from two sources: the semi-infinite extent of the state-space (not just $M = 1, 2$, but M going over all positive integers from 0 to ∞) and the square root M-dependence of the matrix elements of the system–bath interaction assumed

linear in the oscillator displacement for simplicity in a Taylor expansion sense. The practical relevance and usefulness of the studies presented for the vibrational relaxation are clear in light of an enormous experimental literature that exists on that subject.[1–16,19,20] A quite different system that can also be considered as a realistic extension of the nonresonant dimer suggests itself. Because the system has an energy spectrum that is not bounded below, it does not approach thermal equilibrium. Yet it is similar to the relaxing oscillator, its GME can be solved explicitly and *short*-time conclusions that are interesting can be drawn. We describe that system in this section.

The system is an electric charge (for instance an electron or hole) moving among the sites (M, N, etc.) of a one-dimensional crystal lattice of intersite spacing a to which a strong electric field has been applied. The product of the charge, the spacing a and the electric field will be denoted by the symbol $\mathcal{E}$. Known widely as the Wannier–Stark ladder system, the eigenstates are known[51–54] to be localized around the sites of the crystal. Let us consider the system in the simplified one-band form, and assume the bath interaction to connect only nearest-neighbor sites with no dependence on the site label. This system is then less complex than the harmonic oscillator system analyzed for vibrational relaxation because the matrix elements are independent of the site index M but more complex in that the manifold of states extends from $-\infty$ to $+\infty$.

Inspection of the end of Appendix A shows that the GME for $P_M(t)$, the probability of occupation of the Mth Wannier–Stark ladder state (or site), is rather simple since

$$Y_{MN}(z) = \left[\frac{Y_s(z)}{1+e^{-\beta z}}\right][\delta_{N,M+1} + \delta_{N,M-1}].$$

Specifically, the GME is

$$\frac{1}{\kappa}\frac{dP_M(t)}{dt} = \int_0^t dt' \phi_\Delta(t-t')[P_{M-1}(t') - P_{M+1}(t')] + \int_0^t dt' \phi_S(t-t')[P_{M+1}(t') + P_{M-1}(t') - 2P_M(t')], \tag{26}$$

which is nothing but the discrete counterpart of the well-known advective–diffusion equation with memories introduced into it, ϕ_Δ for the advective term and ϕ_S for the diffusive term.

Solutions are entirely straightforward via discrete Fourier transforms. The probability for an initial localized condition $P_M(0) = \delta_{M,0}$ may be written in the Laplace domain, with the understanding that the $\pm$ in the first factor of the denominator is $+$ for positive M and $-$ for negative M, as

$$\widetilde{P}_M(\epsilon) = \frac{\left[\left(\frac{\epsilon}{\kappa} + \widetilde{\phi}_S + \sqrt{\widetilde{\phi}_S^2 - \widetilde{\phi}_\Delta^2}\right)^{1/2} - \left(\frac{\epsilon}{\kappa} + \widetilde{\phi}_S^2 - \sqrt{\widetilde{\phi}_S - \widetilde{\phi}_\Delta^2}\right)^{1/2}\right]^{|M|}}{\left[\widetilde{\phi}_S \pm \widetilde{\phi}_\Delta\right]^{|M|}\left[(\frac{\epsilon}{\kappa} + \widetilde{\phi}_S)^2 + \widetilde{\phi}_\Delta^2 - \widetilde{\phi}_S^2\right]^{1/2}}. \tag{27}$$

The moment expressions are also explicitly given in the Laplace domain from Eq. (27). The expression for an arbitrary moment $\langle M^n \rangle$ is

$$\widetilde{\langle M^n \rangle} = \sum_{\substack{p=0 \\ n-p \text{ even}}}^{n-1} \binom{n-1}{p} \widetilde{\phi}_S(\epsilon) \frac{\kappa \widetilde{\langle M^p \rangle}}{\epsilon} + \sum_{\substack{p=0 \\ n-p \text{ odd}}}^{n-1} \binom{n-1}{p} \widetilde{\phi}_\Delta(\epsilon) \frac{\kappa \widetilde{\langle M^p \rangle}}{\epsilon}, \tag{28}$$

the particular cases of the first and second moments being given by

$$\widetilde{\langle M \rangle} = \frac{\kappa \widetilde{\phi}_\Delta(\epsilon)}{\epsilon^2}, \tag{29a}$$

$$\widetilde{\langle M^2 \rangle} = \frac{\kappa \widetilde{\phi}_S(\epsilon)}{\epsilon^2} + 2\frac{(\kappa \widetilde{\phi}_\Delta(\epsilon))^2}{\epsilon^3}. \tag{29b}$$

Both these expressions clearly reduce to their well-known respective values in the extreme coherent and incoherent limits.

Although Eqs. (29) can be formally inverted, we have not displayed the result as the time-domain expressions bestow no additional clarity. For illustrative purposes we use one of the bath spectral functions we have derived, the Lorentzian, Eq. (37), as an example. As discussed in Sec. 4, the spectral functions are specified by the thermal energy $k_B T$ and the width of the symmetrical spectral function w. For this particular case, the time-domain expression for the velocity of the charge is given by

$$\langle v \rangle = \left(\frac{1 + e^{-\beta \mathcal{E}}}{\pi} \right) t \int_{-\infty}^{\infty} dz \left[\frac{\mathcal{E}^2 + w^2}{z^2 + w^2} \right] \tanh(\beta z/2) \, \mathrm{sinc}[(z - \mathcal{E})t], \tag{30}$$

and that for the mean-squared displacement (MSD) is

$$\begin{aligned} \langle \Delta M^2 \rangle = & \left(\frac{1 + e^{-\beta \mathcal{E}}}{\pi} \right)^2 \iint_{-\infty}^{\infty} dz dz' \left[\frac{\mathcal{E}^2 + w^2}{z^2 + w^2} \right] \left[\frac{\mathcal{E}^2 + w^2}{z'^2 + w^2} \right] \\ & \times (F_2(z, z', t) - F_1(z, t) F_1(z', t)) \\ & + \left(\frac{1 + e^{-\beta \mathcal{E}}}{2\pi} \right) \int_{-\infty}^{\infty} dz \left[\frac{\mathcal{E}^2 + w^2}{z^2 + w^2} \right] t^2 \, \mathrm{sinc}^2 \, \frac{(z - \mathcal{E})t}{2}, \end{aligned} \tag{31}$$

where

$$F_1(z, t) = \left(\frac{t^2}{2} \right) \mathrm{sinc}^2 \, \frac{(z - \mathcal{E})t}{2} \left(\tanh \frac{\beta z}{2} \right),$$

$$F_2(z, z', t) = t^2 \left(\frac{\mathrm{sinc}^2 \, \frac{(z-\mathcal{E})t}{2} - \mathrm{sinc}^2 \, \frac{(z-\mathcal{E})t}{2}}{(z' - z)(z' + z - 2\mathcal{E})} \right) \left(\tanh \frac{\beta z'}{2} \right),$$

$\mathrm{sinc}\, y$ being the function $\sin(y)/y$.

In Fig. 2 we depict the average velocity of the charge, Eq. (30), for $\mathcal{E} = 1$, $\beta = 1/4$ and three values of the spectral width $w = 1/16, 1/4, 2$ in mutually compatible (arbitrary) units. Incoherent and coherent limits of the velocity of the charge are depicted with circles and crosses, respectively. The horizontal axis is

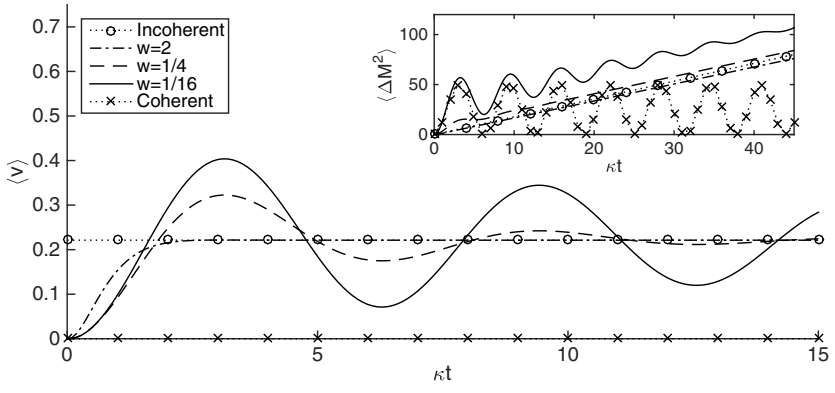

Fig. 2. Transition from coherent quantum localization to incoherent classical delocalization. Depicted is the average velocity of the charge $\langle v \rangle$, Eq. (30), main figure, and the average-squared displacement, Eq. (31), inset, for the dimensionless frequencies/energies $\mathcal{E} = 1$, $k_B T = 4$ and three values of the spectral width $w = 1/16, 1/4, 2$ as well as the coherent and incoherent limits. In the case of arbitrary coherence, the charge initially remains at rest before a delayed acceleration. This contrasts with its counterpart in the incoherent limit which instantaneously achieves its steady-state value $\kappa(1 - \exp(-\beta\mathcal{E}))$. The average-velocity approaches its value in the incoherent limit at long times. The effect of arbitrary coherence is similar for the average-squared displacement (inset) as well: at short times the extent of the charge oscillates as in the coherent case while at long times it is purely diffusive as in the incoherent case.

the dimensionless time κt. At intermediate times, the velocity oscillates around the incoherent steady-state value. As the spectral width is decreased these oscillations persist for a longer period. The increase in the coherence time also results in a longer delay in the initial motion of the charge corresponding to its localization. For arbitrary coherence, the initial motion of the charge is similar to its behavior in the coherent limit. The charge is initially at rest before the electric field acts to accelerate it. The initial dynamics contrasts with the extreme incoherent limit, in which the charge instantaneously accelerates to its final velocity. After the oscillations are damped, the velocity equals $\kappa(1 - \exp(-\beta\mathcal{E}))$ for all values of w. This is expected from the Markoffian approximation to Eq. (29a).

The MSD of the charge, given by Eq. (31), is displayed in the inset of Fig. 2 for the dimensionless energies $\mathcal{E} = 1$, $\beta = 1/4$ and three values of the spectral width $w = 1/16$, $1/4$, 2 along with the MSD in the incoherent (circles) and coherent (crosses) limits. The particle initially "breathes" in the coherent limit as expected from quantum mechanics. These oscillations damp away more quickly as w is increased. The "breathing" frequency depends on the strength of the electric field, with a larger $\mathcal{E}$ corresponding with an increase in the frequency. At long times, the thermalization of the reservoir causes the charge to escape the region of initial localization.

4. Explicit Memory Functions for Specified Baths

We give here some explicit forms of the bath spectral function $Y(z)$ and their resulting memories $\phi(t)$. The detailed balance requirement, which results in bath spectral

functions of the form given in Eq. (3), allows $Y(z)$ to be specified through the symmetrical function $Y_s(z)$. In the simplest cases, the bath can be simply characterized by two energy parameters, the width of the symmetrical spectral function, which we call w, and the thermal energy of the bath which we represent by the inverse temperature $\beta = 1/k_B T$. The system may have various characteristic energies. Let us typify them in the two-state system by the energy difference 2Δ between the two levels, in the Wannier–Stark ladder by the energy difference $\mathcal{E}$ between neighboring sites and in the harmonic oscillator by the frequency Ω of the oscillator. In this section, we use the symbol Ω as the characteristic energy of the system. We remind the reader that energies are normalized by $\hbar\kappa$.

4.1. *Effect of decoherence on memories*

Consider first the triple delta-function, and its approximation with three Lorentzian functions, which we introduce to elucidate the transition from coherent evolution to incoherent. The delta-function triplet peaks at 0 and $\pm\Omega$. Here, in contrast to all the other cases to be treated below, we have normalized $Y(z)$ by setting its integral to 1, given the presence of the δ-function at Ω. The bath spectral function is

$$Y(z) = \frac{2}{1+e^{-\beta z}} \left(H\delta(z) + (1-H)\frac{\delta(z-\Omega)+\delta(z+\Omega)}{2} \right), \tag{32}$$

with H determining the relative strengths of the zero-energy and Ω-energy transitions. The memories $\kappa\phi_{\pm}(t)$ are then found to be proportional to

$$H\cos\Omega t + (1-H)\left[\cos^2\Omega t \mp \left(\tanh\frac{\beta\Omega}{2}\right)\sin^2\Omega t\right].$$

Figure 3 in the left panel displays two examples each of the memories plotted against the dimensionless time κt. The dashed line is $\phi_+(t)$ and the dashed-dotted line is $\phi_-(t)$ for $\beta = 1/2$. The solid line is $\phi_+(t)$ and the dotted line is $\phi_-(t)$ for $\beta = 2$. We take the characteristic system energy $\Omega = 1$ and the spectral strength $H = 1/2$ in both. Both cases illustrate that a spectrum limited to delta-functions results in purely oscillatory memories, and, therefore, in completely coherent motion.

Broadening of the delta-functions in the spectrum by Lorentzians

$$\delta(z) \to \frac{1}{\pi}\left(\frac{\alpha}{z^2+\alpha^2}\right),$$

where α is the broadening (width) parameter, leads to the damping of the memories as expected. Figure 3 in its right panel depicts these damped memories for two values of α. The thermal energy scale is $\beta = 1/2$ in these plots. The dotted and solid lines show the memories, $\phi_+(t)$ and $\phi_-(t)$, respectively, for $\alpha = 1/8$; the coherent oscillations persist for several periods before the memories decay. By contrast, for larger α $(= 1)$, the dashed-dotted and dotted lines depict the respective memories getting damped much quicker. The delta-function spectrum and coherent memories are recovered in the limit $\alpha \to 0$.

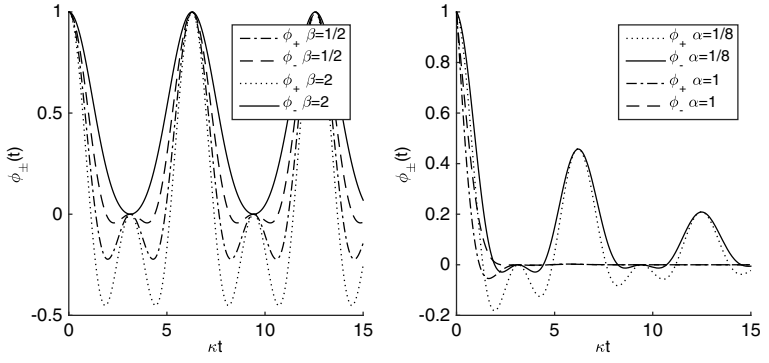

Fig. 3. Time evolution of the memories $\phi_\pm$ for the three-peaked spectral function. Coherent oscillations are seen for true delta-functions in the left panel while the introduction of α, which broadens the delta-functions into Lorentzians, damps the memories in the right panel. Each memory is shown for two values of the thermal energy: $\beta = 1/2$, 2. The right panel depicts the memories that result when each delta-function in Eq. (32) is represented with Lorentzians of finite width α: 1/8 and 1, respectively.

4.2. *Effect of temperature on the spectral function*

In order to understand the effect of temperature on the shape of the spectral function, we show Fig. 4, in which the Gaussian spectral function,

$$Y(z) = \left[\frac{1}{1+e^{-\beta z}}\right] e^{-\frac{z^2}{w^2}},$$

is displayed for four values of the dimensionless energy ratio $\beta\Omega = 0$, 1, 4, ∞. The interval between the solid vertical lines indicates the width of the spectral function and the horizontal axis is normalized by Ω. For very high temperatures, the spectral function is symmetric (solid line). An increase in the parameter $\beta\Omega$ leads to a

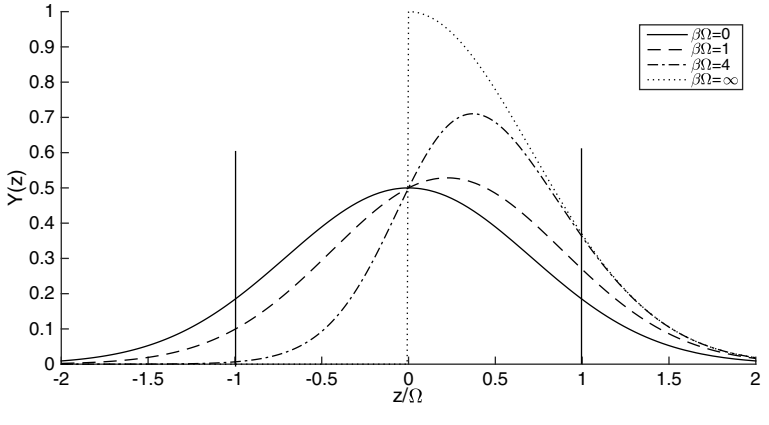

Fig. 4. Gaussian bath spectral function $Y(z)$ is displayed for 4 values of the parameter $\beta\Omega = 0, 1, 4, \infty$. The vertical lines indicate the width of the spectral function and we use Ω to normalize the horizontal axis.

loss of this symmetry in keeping with detailed balance between the energetically upward and downward transitions, respectively. While for small values of $\beta\Omega$ (high temperatures) the spectral function is approximately a Gaussian ($\beta\Omega = 1, 4$) shifted by small extents rightward, for high values (low temperatures) the function tends to a half-Gaussian, being nonnegligible only for positive values of z (dotted line).

4.3. *A catalog of spectral functions and resultant memories*

Having focused on the important effects of damping and of temperature individually, we present, in the rest of this section, a catalog of several spectral functions and their consequent memories. They should be useful for the analysis of coherence not only in vibrational relaxation but in molecular crystals as well.[56,57] We study seven cases, grouped in three. Two examples of a simple truncated spectrum are provided by the flat box and the triangle. The last five consist of simple one-parameter functions with infinite support: the Lorentzian, squared Lorentzian, quartic, mod exponential and the Gaussian already referred to above. Each bath spectrum function is normalized such that $Y(\Omega) = 1/\pi$.

4.3.1. *Spectral functions with compact support, i.e., vanishing outside a finite interval*

To satisfy detailed balance, the width w must be taken as greater than Ω for truncated spectra. The "box" spectral function, centered at the origin, has width $2w$ and constant height $1/\pi$. The expression for $Y(z)$ is given by

$$Y(z) = \frac{1}{\pi}\left[\frac{1+e^{-\beta\Omega}}{1+e^{-\beta z}}\right]\Theta(w-|z|), \tag{33}$$

where $\Theta(z)$ is the Heaviside step function. The memories are

$$\begin{aligned}\phi_{\pm}(t) =& \frac{1+e^{-\beta\Omega}}{\pi}\left[\frac{\sin wt}{t}\cos\Omega t \mp \frac{1-\cos wt}{t}\sin\Omega t\right.\\ &\mp 2\sin\Omega t\sum_{n=1}^{\infty}(-1)^n\left[\left(\frac{t}{n^2\beta^2+t^2}\right)(1-e^{-n\beta w}\cos wt)\right.\\ &\left.\left.-\left(\frac{n\beta}{n^2\beta^2+t^2}\right)e^{-n\beta w}\sin wt\right]\right].\end{aligned} \tag{34}$$

The sum $\phi_S(t) = \phi_-(t) + \phi_+(t)$ and difference $\phi_\Delta(t) = \phi_-(t) - \phi_+(t)$ of the memories given by Eqs. (34) are depicted in the upper left panel of Fig. 5, while the bath spectral function for the "box," Eq. (33), is shown in the inset. The chosen parameter values are: thermal energy $\beta = 1/2$, the characteristic system energy $\Omega = 1$ and the spectral width $w = 4$. The discontinuous spectrum results in memories with persistent oscillations.

The triangular spectral function is centered at the origin with width $2w$, height $w/(w-\Omega)$ and constant slope. The bath spectral function is given by

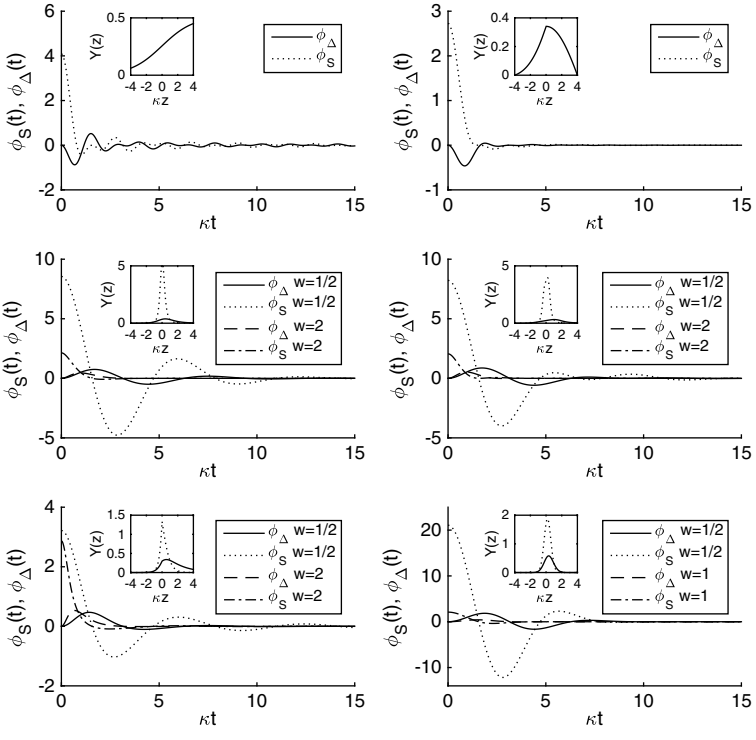

Fig. 5. Depicted in all six panels are the sum and difference of the memories; the inset displays the corresponding bath spectral function. In the upper left panel, we show those of the "box" spectral function, given in Eqs. (34), while in the upper right panel we have those of the triangular spectral function, Eqs. (36). Parameters are $\Omega = 1$, $\beta = 1/2$ and $w = 4$. In the central left and right panels, the memories that arise from a squared Lorentzian and quartic spectral functions, Eqs. (43) and (45), respectively, are shown. Parameters are $\Omega = 1$, $\beta = 1$ and two values $w = 1/2$, 2. In the lower left panel, the memories corresponding to the mod exponential spectral function, Eqs. (47), are displayed while the lower right panel displays the memories, Eqs. (49), for the Gaussian spectral function. Here, $\Omega = 1$ and $\beta = 1$ for both while the spectral width is $w = 1/2$, 2 for the mod exponential and $w = 1/2$, 1 for the Gaussian.

$$Y(z) = \frac{1}{\pi}\left[\left(\frac{1+e^{-\beta\Omega}}{1+e^{-\beta z}}\right)\left(\frac{w-|z|}{w-\Omega}\right)\right]\Theta[w-|z|]. \tag{35}$$

The expression for the memories are therefore

$$\begin{aligned}\phi_\pm(t) = \frac{1+e^{-\beta\Omega}}{\pi(w-\Omega)}\Bigg[&\left(\frac{1-\cos wt}{t^2}\right)\cos\Omega t \mp \left(\frac{wt-\sin wt}{t^2}\right)\sin\Omega t \\ &\mp 2\sin\Omega t\sum_{n=1}^{\infty}(-1)^n\left[\frac{wt}{\beta^2n^2+t^2} - 2n\beta t\left(\frac{1-\cos wt\, e^{-n\beta w}}{(n^2\beta^2+t^2)^2}\right)\right. \\ &\left. - 2t^2\left(\frac{\sin wt\, e^{-n\beta w}}{(n^2\beta^2+t^2)^2}\right)\right]\Bigg].\end{aligned} \tag{36}$$

The upper right panel of Fig. 5, depicts the sum and difference of the memories, Eqs. (34), for the triangular spectra while the spectral function, Eq. (33), is in the inset. Parameter values are $\Omega = 1$, $\beta = 1/2$ and $w = 4$. Compared to the memories that result from the "box" spectral function, those of the triangular $Y(z)$ have weaker oscillations; however, in both cases, the sharp truncation causes persistent oscillations.

4.3.2. *Spectral functions with infinite support*

The Lorentzian spectral function, centered at the origin with spectral width w, results in memories that are particularly simple. The normalized expression for the bath spectral function is given by

$$Y(z) = \left(\frac{1}{\pi}\right)\left(\frac{1+e^{-\beta\Omega}}{1+e^{-\beta z}}\right)\left[\frac{\Omega^2+w^2}{z^2+w^2}\right]. \tag{37}$$

The expressions for the memories that result from Eq. (37) are

$$\phi_{\pm}(t) = \left(\frac{1+e^{-\beta\Omega}}{2}\right)\left(\frac{\Omega^2+w^2}{w}\right)\left[\left(\cos\Omega t \mp \tan\frac{\beta w}{2}\sin\Omega t\right)e^{-wt} \mp 4\sin\Omega t\sum_{n=0}^{\infty}\left[\frac{\beta w}{\beta^2 w^2-\pi^2(2n+1)^2}\right]e^{\frac{-\pi(2n+1)t}{\beta}}\right]. \tag{38}$$

Figure 6, in its left panel, depicts the sum and difference of the memories, Eq. (38), for two sets of the parameter values: characteristic system energy $\Omega = 1$, thermal energy $\beta = 1$ and spectral widths $w = 1/4$ and 4. An increase in the spectral width leads to an increase in the damping of the memories. The inset displays Lorentzian spectral functions that correspond to the characteristic energies above. They are represented by solid and dashed-dotted lines, respectively. An increase in the spectral width both broadens and shifts the bath spectral function.

The Lorentzian spectral function, Eq. (37), can be approximated for small values of βw by a shifted Lorentzian with shift parameter $\bar{z} = \beta w/4$. The width of the approximated Lorentzian spectral function $Y^a(z)$ is modified such that $w \to w(1-\bar{z}^2)$. It is then given by

$$Y^a(z) = \left(\frac{1+e^{-\beta\Omega}}{2\pi}\right)\frac{\Omega^2+w^2}{(z-w\bar{z})^2+w^2(1-\bar{z}^2)^2}. \tag{39}$$

The approximate spectra from Eq. (39) have been introduced because they lead to memories $\phi^a_{\pm}(t)$ that are somewhat simpler than the true memories, Eqs. (38). They are given by

$$\phi^a_{\pm}(t) = \left(\frac{1+e^{-\beta\Omega}}{2}\right)\left(\frac{\Omega^2+w^2}{w(1-\bar{z}^2)}\right)\cos\left(\Omega \pm w\bar{z}\right)t\, e^{-w(1-\bar{z}^2)t}, \tag{40}$$

and might be used for back-of-the-envelope calculations. The difference between the real and approximate memories, Eqs. (38) and (40), respectively, is depicted in the right panel of Fig. 6. Shown are $\phi_{\Delta}(t) - \phi^a_{\Delta}(t)$ and $\phi_S(t) - \phi^a_S(t)$. The characteristic

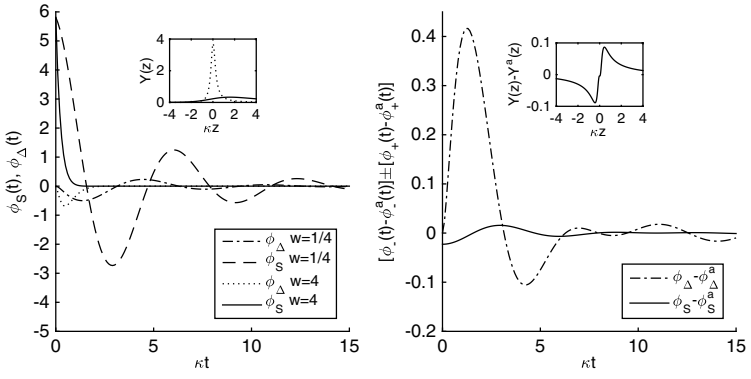

Fig. 6. The left panel displays the sum and the difference of the memories for a Lorentzian spectral function, given in Eqs. (38). In the inset is the corresponding $Y(z)$, Eq. (37). Here $\Omega = 1$, $\beta = 1$ in both and two values of $w = 1/4$, 4 are shown. An increase in the spectral width leads to a broadening of the spectrum (solid line in the inset) and an increase in the damping. Depicted in the right panel are the difference between the real and approximated memories $[\phi_-(t) - \phi_-^a(t)] - [\phi_+(t) - \phi_+^a(t)]$ for a single set of parameter values: $\Omega = 1$, $\beta = 1$ and $w = 1/4$. In the inset is the difference between the corresponding real and approximate bath spectral functions $Y(z) - Y^a(z)$. Note the difference in scale for the left and right panels.

energies are taken to be the same as the first pair of memories ($\Omega = 1$, $\beta = 1$ and $w = 1/4$). The approximate bath spectral function, Eq. (39), differs from the true Lorentzian spectral function closest to the origin (see inset of Fig. 6).

A generalization of the Lorentzian spectral function in Eq. (37) is the generalized Cauchy distribution[55] specified by the parameter ν which determines the high-energy tails of the bath spectral function. The general expression is given by

$$Y(z;\nu) = \left(\frac{1}{\pi}\right)\left(\frac{1+e^{-\beta\Omega}}{1+e^{-\beta z}}\right)\left[\frac{\Omega^2+w^2}{z^2+w^2}\right]^{\nu}, \tag{41}$$

where $\nu > 1/2$ is required for $Y(z,\nu)$ to be normalizable. The Lorentzian spectral function, Eq. (37), re-emerges when $\nu = 1$. Here, we give the case of $\nu = 2$, the square Lorentzian spectral function. This results in a z^{-4}-dependence at high energies. For this case, the generalized spectral function, Eq. (41), is specialized to

$$Y(z) = \left(\frac{1}{\pi}\right)\left(\frac{1+e^{-\beta\Omega}}{1+e^{-\beta z}}\right)\left[\frac{\Omega^2+w^2}{z^2+w^2}\right]^{2}. \tag{42}$$

The memories that result from Eq. (42) are given by

$$\begin{aligned}\phi_\pm(t) = &\left(\frac{1+e^{-\beta\Omega}}{4}\right)\left(\frac{\Omega^2+w^2}{w^{\frac{3}{2}}}\right)^2 \\ &\times\left[\frac{(1+wt)(\cos\Omega t+\cos(\Omega t\pm\beta w))\pm\beta w\sin\Omega t}{1+\cos\beta w}e^{-wt}\right. \\ &\left.\mp 8\sin\Omega t\sum_{n=0}^{\infty}\left[\frac{\beta^3w^3}{(\beta^2w^2-\pi^2(2n+1)^2)^2}e^{-\frac{\pi(2n+1)t}{\beta}}\right]\right].\end{aligned} \tag{43}$$

The bath spectral function, Eq. (42), and the sum and difference of the memories, Eq. (43), are displayed in the central left panel of Fig. 5, for $\Omega = 1$, $\beta = 1$ and $w = 1/2$, 2. The bath spectral function (inset) shows the standard broadening and shifting as the spectral width w is increased.

As a comparison, the quartic spectral function possesses a z^{-4}-dependence at high energies as well. The expression for its bath spectral function is

$$Y(z) = \left(\frac{1}{\pi}\right)\left(\frac{1+e^{-\beta\Omega}}{1+e^{-\beta z}}\right)\left[\frac{\Omega^4+w^4}{z^4+w^4}\right]. \tag{44}$$

The distinction between the squared Lorentzian spectral function, Eq. (42), and Eq. (44) is most evident in the intermediate energy regime. The memories that result from Eq. (44) are given by

$$\begin{aligned}\phi_{\pm}(t) = \left(\frac{1+e^{-\beta\Omega}}{\sqrt{8}}\right)\left(\frac{\Omega^4+w^4}{w^3}\right)\Bigg[&\left(\cos\frac{wt}{\sqrt{2}}+\sin\frac{wt}{\sqrt{2}}\right)\cos\Omega t\, e^{-\frac{wt}{\sqrt{2}}} \\ &\mp\left[\left(\frac{\sinh\eta+\sin\eta}{\cosh\eta+\cos\eta}\right)\sin\frac{wt}{\sqrt{2}}-\left(\frac{\sinh\eta-\sin\eta}{\cosh\eta+\cos\eta}\right)\cos\frac{wt}{\sqrt{2}}\right]\sin\Omega t\, e^{-\frac{wt}{\sqrt{2}}} \\ &\mp 4\sqrt{2}\sin\Omega t\sum_{n=0}\left[\frac{\beta^3w^3}{\beta^4w^4+\pi^4(2n+1)^4}e^{-\frac{\pi(2n+1)t}{\beta}}\right]\Bigg].\end{aligned} \tag{45}$$

Here $\eta = \beta w/\sqrt{2}$. The sum and difference of the quartic spectral function memories, Eqs. (43), are depicted for $\Omega = 1$, $\beta = 1$ and $w = 1/2$ and 2 in the central right panel of Fig. 5, with $Y(z)$, Eq. (42), in the inset.

The mod exponential spectral function is centered at the origin with width w. Its bath spectral function is given by

$$Y(z) = \left(\frac{1}{\pi}\right)\left(\frac{1+e^{-\beta\Omega}}{1+e^{-\beta z}}\right)e^{-\frac{|z|-\Omega}{w}}. \tag{46}$$

The memories that result from Eq. (46) are expressed as

$$\begin{aligned}\phi_{\pm}(t) = \left(\frac{1+e^{-\beta\Omega}}{2\pi}\right)we^{\frac{\Omega}{w}}\Bigg[&\frac{\cos\Omega t\mp wt\sin\Omega t}{1+w^2t^2} \\ &\mp 4\sin\Omega t\sum_{n=1}^{\infty}(-1)^n\frac{wt}{(1+n\beta w)^2+w^2t^2}\Bigg]\end{aligned} \tag{47}$$

The sum and difference of the memories, Eqs. (47), are depicted in the bottom left panel of Fig. 5. The parameter values $\Omega = 1$, $\beta = 1$ and two values of $w = 1/2$, 2 are considered. Inset is the mod exponential spectral function in dotted and solid lines, respectively. The discontinuity in the derivative of the exponential spectral function at $z = 0$ causes the oscillations to be persistent.

The final bath spectral function we consider is a Gaussian of width w already referred to in our elucidation of temperature effects:

$$Y(z) = \left(\frac{1}{\pi}\right)\left(\frac{1+e^{-\beta\Omega}}{1+e^{-\beta z}}\right)e^{-\frac{z^2-\Omega^2}{w^2}}. \tag{48}$$

The magnitude of Eq. (48) is strongly dependent on the width. The memories that result from a Gaussian spectral function are given by

$$\phi_{\pm}(t) = \frac{1+e^{-\beta\Omega}}{4}\frac{we^{\frac{\Omega^2}{w^2}}}{\sqrt{\pi}}\left[e^{-\frac{w^2t^2}{4}}\cos\Omega t \pm i\left(\mathrm{w}\left(\frac{wt}{2}\right) - \mathrm{w}\left(-\frac{wt}{2}\right)\right)\sin\Omega t\right.$$
$$\left. + 2i\sin\Omega t\sum_{n=1}(-1)^n\left(\mathrm{w}\left(\frac{wt+in\beta w}{2}\right) - \mathrm{w}\left(\frac{-wt+in\beta w}{2}\right)\right)\right]. \quad (49)$$

The Fourier transform of Eq. (48) results in a scaled error function of complex argument which we represent with the Faddeeva function,[58] $\mathrm{w}(iz) = \exp(z^2)\mathrm{erfc}(z)$. The presence of i in Eq. (49) should not lead the reader to conclude the memories have imaginary components. As shown in the bottom right panel of Fig. 5, they are certainly real. Depicted are the sum and difference of the memories for $\Omega = 1$, $\beta = 1$ and two values of $w = 1/2$ and 1 with the corresponding $Y(z)$ inset with, respectively, dotted and solid lines.

When the dimensionless energy ratio βw is small, the Gaussian spectral function can be approximated with a shifted Gaussian centered at $w(1-\bar{z}^2)$ where $\bar{z} = \beta w/4$. The approximation to the bath spectral function, Eq. (48), is given by

$$Y^a(z) = \frac{1}{\pi}\frac{1+e^{-\beta\Omega}}{2}e^{-\frac{\Omega^2}{w^2}}e^{-\frac{(z-w\bar{z})^2}{w^2(1-\bar{z}^2)^2}}. \quad (50)$$

The exact memories for the approximate spectral function, Eq. (50), provide an analytically tractable approximation for calculations. They are given by

$$\phi^a_{\pm}(t) = \frac{w(1-\bar{z}^2)}{\sqrt{\pi}}\frac{1+e^{-\beta\Omega}}{2}e^{\frac{\Omega^2}{w^2}}\cos\left(\Omega \pm w\bar{z}\right)t\, e^{-w^2(1-\bar{z}^2)^2t^2} \quad (51)$$

4.4. *Physical discussion of memory behavior*

The behavior of the memories for particular bath spectral functions is intimately related to the relative values of the three (dimensionless) energies that characterize the system and the reservoir: the system energy Ω, the thermal energy of the bath $1/\beta$ and w, the energy that characterizes the spectral resolution of the bath. Physically, the effects caused by the variation of these parameters are related to the change in the ratios of the energy scales, βw, $\beta\Omega$ and Ω/w. The first ratio compares the thermal energy of the reservoir to its average spectral energy. The second and third ratios compare the respective reservoir energies to the system energy. Small values of either lead to incoherent motion. The exchange of energy is suppressed when the ratios are large, which extends the time scale of coherent system evolution.

It may be useful to discuss the effects on the memories directly in terms of changes in the underlying energies. We do this in Figs. 7–9. In all the three figures, we display the memories that result from a Lorentzian spectral function, Eq. (37), and have set the time scale with κ.

In Fig. 7, we display the effects of varying the characteristic energy of the system Ω on the memories. Two values, $\Omega = 1/2$ and $\Omega = 2$, are shown for three pairs of

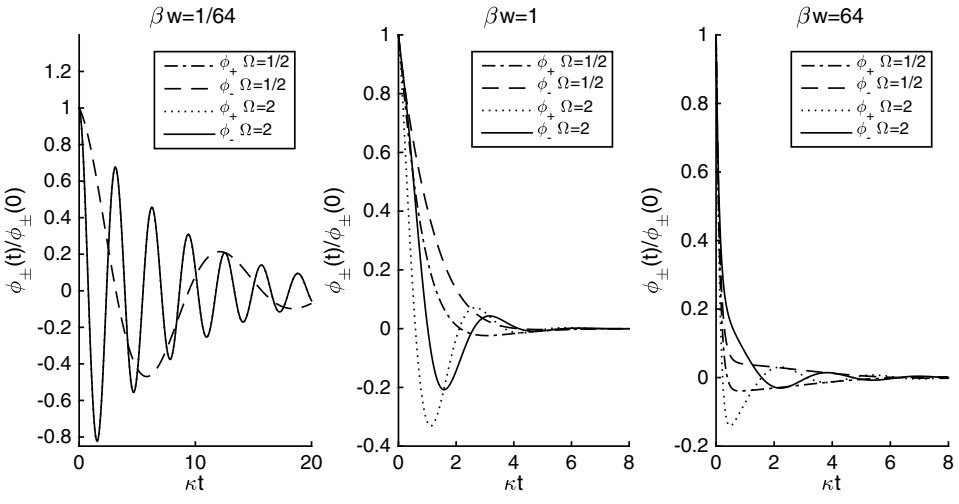

Fig. 7. The normalized memories, $\phi_\pm(t)/\phi_\pm(0)$, for the Lorentzian spectral function are shown for two values of Ω in each of the panels. From left to right, the ratio of the characteristic reservoir energies, βw, takes the values $\beta w = 1/64$ ($\beta = 1/8$, $w = 1/8$), $\beta w = 1$ ($\beta = 1$, $w = 1$) and $\beta w = 64$ ($\beta = 8$, $w = 8$). The increase in Ω increases the oscillation frequency of the memories and, therefore, the coherence time of the system evolution.

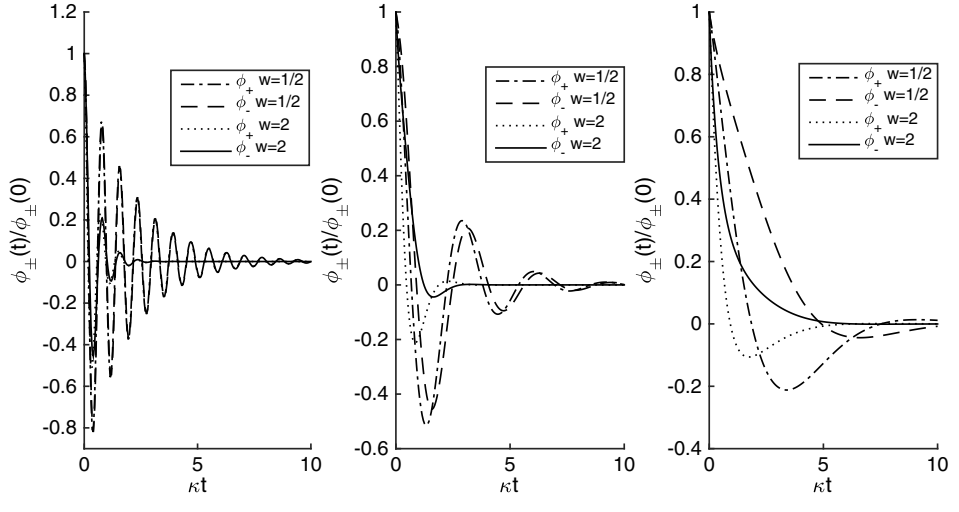

Fig. 8. A variation to the spectral energy, at $w = 1/2,\ 2$, is displayed for the case of the Lorentzian spectral function. Three pairs of the ratio of the characteristic system energy to the thermal energy of the reservoir are shown: ($\Omega = 8$, $\beta = 1/4$), ($\Omega = 2$, $\beta = 1$) and ($\Omega = 1/4$, $\beta = 8$). The ratio $\beta\Omega = 2$ is held constant. An increase in the spectral width w generally results in an increase in the damping relative to the oscillation period. However, smaller values of βw decrease the effect as the thermal energy scale begins to dominate the dynamics.

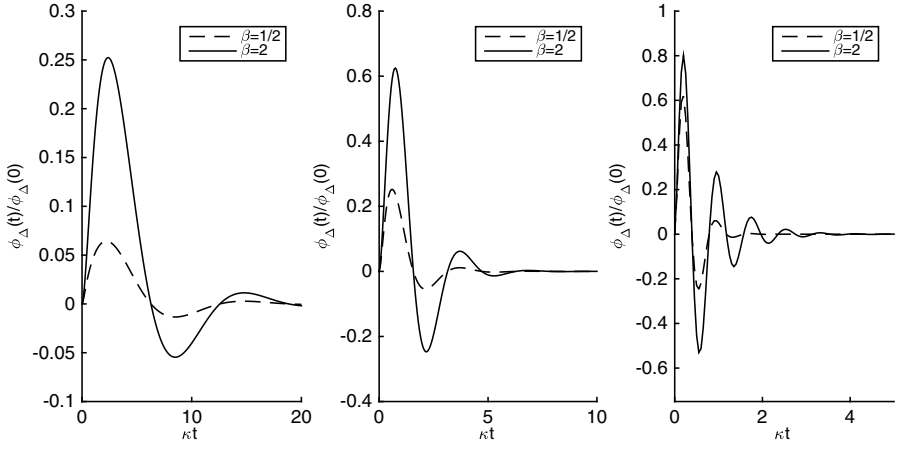

Fig. 9. We display here the difference between the normalized memories, $\phi_-(t)/\phi_-(0) - \phi_+(t)/\phi_+(0)$, against the dimensionless time κt for two values of the thermal energy, $\beta = 1/2,\ 2$, and three pairs of the ratio of the system energy and spectral width: left ($\Omega = 8,\ w = 48$), center ($\Omega = 2,\ w = 1$) and right ($\Omega = 1/4,\ w = 1/8$). Larger values of β result in an increase in the distinction between the memories. However, the effect itself becomes less important as βw decreases commensurately with the increase in the spectral damping.

characteristic reservoir energies: $\beta = 1/8$ and $w = 1/8$ (left), $\beta = 1$ and $w = 1$ (center) and $\beta = 8$ and $w = 8$ (right). The characteristic reservoir energies are chosen to highlight the effect of thermal deviations to the spectra. Generally, an increase of Ω leads to a decrease in the period of oscillation. The left panel displays the parameter regime where neither of the characteristic reservoir energy scales are large compared to the system energy. Thus, the oscillation of the memories persist for multiple periods. An increase to the characteristic reservoir energies, shown in the second panel, results in an increase to the damping strength. However, as seen in the right panel, when βw is large, thermal effects dominate the spectral energies and coherency begins to re-emerge.

The memories for two values of the characteristic spectral energy, $w = 1/2,\ 2$, are displayed in each panel of Fig. 8. The ratio of the characteristic system energy to the thermal energy is held constant: left ($\Omega = 8,\ \beta = 1/4$), center ($\Omega = 2,\ \beta = 1$) and right ($\Omega = 1/4,\ \beta = 8$). As evidenced in Fig. 8, the coherent time scale is decreased when the spectral width w is increased. Small values of w indicate a limit to the capability of the reservoir to dissipate energy. The effect is diminished for small values of βw when the thermal energy scale dominates the behavior of the reservoir.

Figure 9 depicts the effect of a change in β on the difference between the normalized memories $\phi_\pm(t)/\phi_\pm(0)$. This reflects the distinction between transitions to sites at lower energy to those at higher energy. Each panel displays the difference for two values, $\beta = 1/2,\ 2$, while the ratio of the characteristic system energy to the spectral energies is held constant. From left to right, we use ($\Omega = 8,\ w = 4$), ($\Omega = 2,\ w = 1$) and ($\Omega = 1/4,\ w = 1/8$). An increase in the thermal energy leads to

a commensurate increase in the distinguishability of the two memories. However, this effect is damped when the spectral energy scale sets the energy of the reservoir, i.e., when βw is large.

5. Conclusion

Although the analysis reported in this paper targets fundamental questions regarding the approach to equilibrium of any quantum system, its aim is modest. It is not to introduce the generalized master equation or solve the central problem of irreversibility or make understandable closure in nonequilibrium statistical mechanics, all of which have been done (or attempted with a great deal of success) decades ago by masters of the field.[34–43] Even *applications* of the GME, particularly for transport, have been systematically pursued as in the large body of work accumulated in Frenkel exciton transport in molecular crystals.[59] The focus of the present investigation is rather on describing the approach to equilibrium with particular attention paid to the simultaneous occurrence of decoherence and population relaxation; and to use for this purpose simple GMEs obtained in the weak-coupling approximation. The use of the weak-coupling approximation here should be noted as a *desirable* feature rather than a source of apology since, as explained in Sec. 1, the interaction with the bath that one must select is necessarily such that no superfluous signatures of the bath are left in the final state. That final equilibrium state must be given by the double postulate of equilibrium statistical mechanics (that has no reference to the bath other than the value of the temperature, only to the eigenstates of the system) as explained in textbooks.[21]

An analysis similar to the one reported here was initiated briefly in a previous publication[50] where the system was rather elementary, a nonresonant dimer (two-state system with unequal energies of the states). The present study targets considerably more realistic systems: a harmonic oscillator representing a molecule undergoing vibrational relaxation (Sec. 3) and a charged particle moving in a crystal lattice made energetically nondegenerate by the application of a strong electric field. Our study of the first system provides a GME generalization of the well-known Montroll–Shuler equation[9] in chemical physics and thereby extends its applicability to very short times and opens the possibility of practical application in those time ranges.

That work on vibrational relaxation, particularly at short times, reported in Sec. 2 of this paper, is the primary practical goal of our investigation. Recent availability of experimental methods capable of probing the process of vibrational relaxation at shorter and shorter times (the passage of pico- into femto-spectroscopy and now the advent of even faster spectroscopy) should make our study especially relevant in the modern era. We mention, as examples, the work of Zewail and collaborators: femtosecond observation of coherent collisional confinement,[25] of solvated oxygen anions[26] and of anomalies in the vibrational redistribution in azulene.[27]

Specifically, we have generalized the Montroll–Shuler equation (4), a respected workhorse of traditional vibrational relaxation investigations, into the GME (6) along with explicit prescriptions to obtain the memory functions $\phi_{\pm}(t)$ from features of the bath with which the relaxing molecule interacts. The bath features are to be found in the spectral function $Y(z)$. The Fourier-transform prescription obtained by generalizing Zwanzig's projection operators to include coarse-graining is explained in Appendix A and a treatment cataloging various spectral functions and consequent memories by the application of that prescription are provided in Sec. 4. Section 2.3 and Fig. 1 make particularly clear how our theoretical predictions may be compared, in principle, to coherent observations of vibrational relaxation at ultra-short times.

While not the primary goal of our analysis in this paper, the charge in the crystal lattice analyzed in Sec. 3 is a secondary target of our study, included here as it is naturally studied with our methods. It can be viewed as a system that generalizes the elementary example of the nonresonant dimer analyzed by Tiwari and Kenkre[50] by augmenting its two states into an infinite number of states (sites of the crystal). The vibrational relaxation of the molecule analyzed in Sec. 2 is a similar generalization to a semi-infinite number of states (appropriate to the harmonic oscillator spectrum) starting from two in the simple system of Ref. 50 but also with the added complication of the site-dependent matrix elements of the bath interaction Hamiltonian. Our study of the charge under the action of an electric field in a crystal lattice uncovers an interesting transition from coherent behavior at short times, characterized by localization around the initial state, to delocalization at long times as the charge escapes to infinitely distant sites. This is a passage from quantum mechanical motion to classical motion.

The study of several cases of the phenomenological bath is another feature of the present paper. We have calculated the memory functions of our GME for various realizations of the spectral bath function $Y(z)$ and investigated the dependence of the memory functions on the temperature as well as spectral features. The advantage of using phenomenologically modeled baths and consequent spectral functions, as we have done in the present paper, is that it allows the study of complex reservoir interactions which are difficult to model simply but are reflected in independent observations. This is best exemplified by the Förster prescription in the theory of energy transfer[60] where the independent observations are absorption and emission spectra while the phenomena that need to be described are those involving excitation transfer.

Nevertheless, it is also possible to show how to obtain our GME and the memory functions in it *directly* for fully specified *microscopic* models. In cases wherein the interaction term in equations such as Eqs. (A.3) and (A.4) is of the product form $V = V_S V_B$, where the first (second) factor has operators only of the system (bath), the memories can be simplified further. As in Ref. 16, the memory functions, $\mathcal{W}_{MN}(t)$ and $\mathcal{W}_{NM}(t)$, can be written as products of pure system factors and pure

bath correlations $\mathcal{B}(t) = \langle V_B V_B^\dagger(t)\rangle$ and its complex conjugate $\mathcal{B}^*(t) = \langle V_B(t) V_B^\dagger\rangle$:

$$\mathcal{W}_{MN}(t) = |\langle M|V_S|N\rangle|^2 (e^{i\Omega_{MN}t}\mathcal{B}(t) + e^{-i\Omega_{MN}t}\mathcal{B}^*(t)), \tag{52a}$$

$$\mathcal{W}_{NM}(t) = |\langle M|V_S|N\rangle|^2 (e^{-i\Omega_{MN}t}\mathcal{B}(t) + e^{i\Omega_{MN}t}\mathcal{B}^*(t)). \tag{52b}$$

Here $\Omega_{MN} = E_M - E_N/\hbar$ is the frequency defined by the energy difference between the system energy levels M and N; and $|\langle M|V_S|N\rangle|^2$ depends only on the system (not bath). In the case of the degenerate system (no differences in the energies between states, i.e., $\Omega_{MN} = \Omega_{NM} = 0$), the memory functions are found to be equal to each other,

$$\mathcal{W}_{MN}(t) = \mathcal{W}_{NM}(t) = |\langle M|V_S|N\rangle|^2 (\mathcal{B}(t) + \mathcal{B}^*(t)). \tag{53}$$

The bath correlation functions $\mathcal{B}(t)$ and $\mathcal{B}^*(t)$ involve symbols such as $\langle \cdots \rangle$ and $V_B(t)$. These follow the standard notation in textbooks and represent, respectively, the bath thermal average and the Heisenberg time dependence, H_B being the Hamiltonian of the bath. Thus

$$\mathcal{B}(t) = \langle V_B V_B^\dagger(t)\rangle = \frac{\mathrm{Tr}(e^{-\beta H_B} V_B e^{itH_B} V_B^\dagger e^{-itH_B})}{\mathrm{Tr}(e^{-\beta H_B})}. \tag{54}$$

Work with the help of the theory developed here is under way in several further directions. One of them focuses on calculations of the memories and the study of the short-time aspects of relaxation for *microscopically* specified baths via computations of the correlation function given by Eq. (54) appropriate to observations.[4–6,16] Quantum representations of anharmonic reservoirs are also being studied in this context.[61] Another elucidates the effects of initial conditions of molecular excitation or system preparation as described by driven GMEs. Such a treatment is necessary because the analysis we have given here is only applicable for an initial density matrix that is random in the representation of M, N, etc. For situations in which this is not true, the GME must be supplemented by driving terms first derived long ago by van Hove,[34] Zwanzig[35] and others and analyzed in specific contexts.[44] Yet other directions of our current research focus on the understanding of time-*independent* aspects of relaxation observations such as the puzzling inverted temperature dependence of rates reported by Tokmakoff and collaborators.[5] These matters, available in the form of unpublished calculations, will be the contents of a future publication.[62]

Acknowledgments

It is a pleasure to acknowledge helpful discussions with Anastasia Ierides.

Appendix A. Essentials of the Fourier-Transform Prescription to Obtain Coarse-Grained Memories

A minimal description of how to obtain the Fourier-transform prescription[45] originally given by one of the present authors is provided in this Appendix to facilitate

an understanding of the derivation. This appears useful because the original exposition[48] had been in the context of the extension into the coherent domain of the Förster theory[60] of excitation transfer in photosynthetic and related systems and had a sharply specialized emphasis. The derivation uses coarse-grained projection operators introduced as a generalization[45,48,49] to the diagonalization projection operators invented in Refs. 35–38. Starting with the von Neumann equation for the density matrix ρ, we arrive under the guidance of the Zwanzig procedure at the master equation for the probabilities. However, the latter are coarse-grained entities characteristic only of the system, rather than of the system–bath composite, and obtained through a summation over the states of the bath. The summation is built[45,48,49] into the projection operator. Specifically, if M, N, etc. denote the states of the system alone and m, n, p, etc. denote those of the bath, the projection operator $\mathcal{P}$ is defined to act on any operator O, as

$$\langle M,m|\mathcal{P}O|N,n\rangle = \frac{Q_m}{Q}\left[\sum_p \langle M,p|O|M,p\rangle\right]\delta_{M,N}\delta_{m,n}. \tag{A.1}$$

Its action is threefold. The two Kronecker deltas correspond to the fact that $\mathcal{P}O$ is diagonal. The sum coarse-grains over the bath states. Each microstate is weighted through a factor Q_m, idempotency of $\mathcal{P}$ being ensured by the normalization $\sum_m Q_m = Q$. As explained elsewhere,[49] different realizations of the weighting factor Q_m may be used in the coarse-graining for different goals but here we take them as corresponding to the bath thermal distribution proportional to $e^{-\beta\epsilon_m}$. The energy of the mth bath eigenstate is denoted by ϵ_m, and as elsewhere, β is the dimensionless inverse temperature. The rest of the calculation follows Zwanzig's in its essence but removes an important shortcoming by introducing sums over bath states in the very prescription for the memories thereby providing a Fourier-transform recipe to obtain memories from bath spectral functions. We obtain Zwanzig's GME as

$$\frac{dP_M(t)}{dt} = \sum_N \int_0^t dt'[\mathcal{W}_{MN}(t-t')P_N(t') - \mathcal{W}_{NM}(t-t')P_M(t')], \tag{A.2}$$

where $\mathcal{W}_{MN}(t)$ and $\mathcal{W}_{NM}(t)$ are the memories but now directly between coarse-grained states M and N, rather than between single states of the system–bath combination. The memories are given by

$$\mathcal{W}_{MN}(t) = 2\sum_{m,n}\frac{e^{-\beta\epsilon_n}}{Z}|\langle M,m|V|N,n\rangle|^2\cos[(\epsilon_{mn}+E_{MN})t], \tag{A.3a}$$

$$\mathcal{W}_{NM}(t) = 2\sum_{m,n}\frac{e^{-\beta\epsilon_m}}{Z}|\langle M,m|V|N,n\rangle|^2\cos[(\epsilon_{mn}+E_{MN})t], \tag{A.3b}$$

where $E_{MN} = E_M - E_N$ and $\epsilon_{mn} = \epsilon_m - \epsilon_n$ are the differences in energy between the system states and bath states, respectively, and $Z = \sum_n e^{-\beta\epsilon_n}$ is the bath partition function. To get Eq. (A.3b), whose only difference from Eq. (A.3a) is the presence of ϵ_m rather than of ϵ_n in the Boltzmann weighting factor within the

bath summation, we first switch in Eq. (A.3a) labels N with M and n with m and then use the indifference of cosine to the sign of its argument. These expressions correspond with the textbook statement that one performs a thermal average over initial states and a sum over the final states.

We can now again switch indices within the bath summation, use the properties of the cosine and write Eq. (A.3b) in the form

$$\mathcal{W}_{NM}(t) = 2\sum_{m,n} \frac{e^{-\beta\epsilon_n}}{Z} |\langle M, m|V|N, n\rangle|^2 \cos\left[(\epsilon_{mn} - E_{MN})t\right]. \tag{A.4}$$

The distinction between the two memories connecting the coarse-grained states M–N is then wholly in a *sign* in the argument of the cosine. The memory corresponding to the transition from N to M has the difference of ϵ_{mn} and E_{MN} whereas that corresponding to the transition from M to N has their sum.

Consider now a complex system wherein the bath energy differences may be regarded as continuous and denoted by the variable z. We split the unrestricted summation $\sum_{m,n}$ over the bath states into a primed (restricted) summation $\sum'_{m,n}$ with the restriction that ϵ_{mn} equals the value z, followed by an integration over the latter. Equations (A.3) may be written more appropriately in the integral form

$$\mathcal{W}_{MN}(t) = \int_{-\infty}^{\infty} dz\, Y_{MN}(z) \cos\left[(z + E_{MN})t\right], \tag{A.5a}$$

$$\mathcal{W}_{NM}(t) = \int_{-\infty}^{\infty} dz\, e^{-\beta z} Y_{NM}(z) \cos\left[(z + E_{MN})t\right], \tag{A.5b}$$

with Eq. (A.4) becoming

$$\mathcal{W}_{NM}(t) = \int_{-\infty}^{\infty} dz\, Y_{MN}(z) \cos\left[(z - E_{MN})t\right]. \tag{A.6}$$

Several features deserve mention. The quantities $Y_{MN}(z)$ and $Y_{NM}(z)$ contain everything in the summands except the cosines, thus $Y_{MN}(z) = 2[\rho(z)/Z] \sum'_{m,n} e^{-\beta\epsilon_n} |\langle M, m|V|N, n\rangle|^2$, the factor $e^{-\beta z}$ in the second equation appears because of the switch of m and n in the indices in the summands and $\rho(z)$ is the density of states that emerges from the replacement of the summation by an integration.

In systems such as the ones analyzed here, $Y_{MN}(z)$ or $Y_{NM}(z)$ are separable into a product of a system expression and a bath expression. Thus, for the primary situation analyzed in Sec. 2 of the main paper, the harmonic oscillator in interaction with the bath, the system expression is proportional to

$$[\sqrt{M+1}\delta_{N,M+1} + \sqrt{M}\delta_{N,M-1}]^2 = (M+1)\delta_{N,M+1} + M\delta_{N,M-1}.$$

The expression is a consequence of the square root dependence of the matrix element of the system–bath interaction between harmonic oscillator eigenstates and its nearest-neighbor nature in the M, N-space. This is so because the interaction is linear in the oscillator coordinate from the Taylor expansion employed by Landau

and Teller.[47] By contrast, the second system analyzed in the paper, in Sec. 3, the charge under the action of an electric field in a crystal, the system expression of $Y_{MN}(z)$ or $Y_{NM}(z)$ has no similar square root dependence on the system state label but is taken nearest-neighbor and thus proportional simply to $[\delta_{N,M+1} + \delta_{N,M-1}]$.

The other factor in the expression for $Y_{MN}(z)$ or $Y_{NM}(z)$ comes from bath properties. We denote it by $Y(z)$ without the indices M and N, and call it the bath spectral function $Y(z)$. It allows one to focus attention on a phenomenological construction of the bath used in the present paper. The equivalence between Eqs. (A.5b) and (A.6) shown above is an explicit proof of the generalized detailed balance requirement, given in Eq. (2) in the text, that $Y(z)$ respects the relation $Y(-z) = e^{-\beta z}Y(z)$ given in the text or that it can always be represented through a symmetric function as in Eq. (3).

Finally, we can write down the Y_{MN} used in Sec. 2 as

$$Y_{MN}(z) = \left[\frac{Y_s(z)}{1 + e^{-\beta z}}\right][(M+1)\delta_{N,M+1} + M\delta_{N,M-1}], \tag{A.7}$$

and that used in Sec. 3 as

$$Y_{MN}(z) = \left[\frac{Y_s(z)}{1 + e^{-\beta z}}\right][\delta_{N,M+1} + \delta_{N,M-1}]. \tag{A.8}$$

The transition rate κ is given by substituting z in $\kappa = Y_s(z)/(1 + e^{-\beta z})$ by Ω for the harmonic oscillator case in Sec. 2 and $\mathcal{E}$ for the charge in the crystal case in Sec. 3. The phenomenological introduction of any symmetric function for $Y_s(z)$, with assumed z-dependence as discussed for various cases in Sec. 4, completes the full specification of the GMEs, Eqs. (6) and (26), at the respective starting points of Secs. 3 and 4.

References

1. A. Laubereau and W. Kaiser, *Rev. Mod. Phys.* **50**, 605 (1978).
2. S. H. Lin and H. Eyring, *Annu. Rev. Phys. Chem.* **25**, 39 (1974).
3. D. W. Oxtoby, *Annu. Rev. Phys. Chem* **32**, 77 (1981).
4. D. D. Dlott and M. D. Fayer, *J. Chem. Phys.* **92**, 3798 (1990).
5. A. Tokmakoff *et al.*, *Chem. Phys. Lett.* **221**, 412 (1994).
6. A. Tokmakoff, B. Sauter and M. D. Fayer, *J. Chem. Phys.* **100**, 9035 (1994).
7. R. J. Rubin and K. E. Shuler, *J. Chem. Phys.* **25**, 59 (1956); **25**, 68 (1956).
8. R. J. Rubin and K. E. Shuler, *J. Chem. Phys.* **26**, 137 (1957).
9. E. W. Montroll and K. E. Shuler, *J. Chem. Phys.* **26**, 3 (1957).
10. A. Nitzan and J. Jortner, *Mol. Phys.* **25**, 713 (1973).
11. K. F. Freed and D. F. Heller, *J. Chem. Phys.* **61**, 3942 (1974).
12. D. J. Diestler, *Adv. Chem. Phys.* **35**, 305 (1980).
13. S. A. Adelman, R. Muralidhar and R. H. Stote, *J. Chem. Phys.* **95**, 2738 (1991).
14. V. M. Kenkre and V. Seshadri, *Phys. Rev. A* **15**, 197 (1977).
15. V. Seshadri and V. M. Kenkre, *Phys. Rev. A* **17**, 223 (1978).
16. V. M. Kenkre, A. Tokmakoff and M. D. Fayer, *J. Chem. Phys.* **101**, 10618 (1994).
17. F. P. Buff and D. J. Wilson, *J. Chem. Phys.* **32**, 677 (1960).
18. A. H. Zewail, *J. Phys. Chem. A* **104**, 5660 (2000).

19. K. E. Shuler, *Symp. (Int.) Combust.* **5**, 56 (1955).
20. A. Tokmakoff, M. D. Fayer and D. D. Dlott, *J. Phys. Chem.* **97**, 1901 (1993).
21. K. Huang, *Statistical Mechanics* (Wiley, New York, 1987) [see in particular pp. 172–173].
22. W. H. Zurek, S. Habib and J. P. Paz, *Phys. Rev. Lett.* **70**, 1187 (1993).
23. D. Giulini *et al.*, *Decoherence and the Appearance of a Classical World in Quantum Theory* (Springer, Berlin, 1996).
24. W. H. Zurek, *Rev. Mod. Phys.* **75**, 715 (2003).
25. C. Wan *et al.*, *J. Chem. Phys.* **106**, 4353 (1997).
26. E. W.-G. Diau, S. D. Feyter and A. H. Zewail, *J. Chem. Phys.* **110**, 9785 (1999).
27. N. J. Kim, D. H. Paik and A. H. Zewail, *J. Chem. Phys.* **118**, 6930 (2003).
28. S. K. Sundaram and E. Mazur, *Nature Mater.* **1**, 217 (2002).
29. E. Goulielmakis *et al.*, *Nature* **466**, 739 (2010).
30. I. Tehver and V. Hizhnyakov, *Zh. Eksp. Teor. Fiz.* **69**, 599 (1975) [English translation: *Sov. Phys.-JETP* **42**, 305 (1976)].
31. V. M. Kenkre, *Phys. Rev. A* **16**, 766 (1977).
32. H. C. Andersen *et al.*, *J. Math. Phys.* **5**, 522 (1964).
33. H. C. Andersen *et al.*, *J. Chem. Phys.* **41**, 3012 (1964).
34. L. van Hove, *Physica* **23**, 441 (1957).
35. R. Zwanzig, *J. Chem. Phys.* **33**, 1338 (1960).
36. R. Zwanzig, *Lectures in Theoretical Physics*, Vol. 3, eds. W. E. Brittin, B. W. Downs and J. Downs (Interscience, New York, 1961).
37. R. Zwanzig, *Physica* **30**, 1109 (1964).
38. R. Zwanzig, Statistical mechanics of irreversibility, in *Quantum Statistical Mechanics*, ed. P. H. E. Meijer (Gordon and Breach, New York, 1966), p. 139.
39. E. G. D. Cohen (ed.), *Fundamental Problems in Statistical Mechanics: Proc. NUFFIC Int. Summer Course in Science at Nijenrode Castle, the Netherlands, August, 1961*, (North-Holland, Amsterdam, 1962).
40. J. de Boer and G. E. Uhlenbeck, *Studies in Statistical Mechanics*, Vol. 1 (North-Holland, Amsterdam, 1962).
41. E. W. Montroll, in *Fundamental Problems in Statistical Mechanics*, ed. E. G. D. Cohen (North-Holland, Amsterdam, 1962), p. 230.
42. I. Prigogine and P. Résibois, *Physica* **24**, 795 (1958).
43. R. J. Swenson, *J. Math. Phys.* **3**, 1017 (1962).
44. V. M. Kenkre, *J. Stat. Phys.* **19**, 333 (1978).
45. V. M. Kenkre, The generalized master equation and its applications, in *Statistical Mechanics and Statistical Methods in Theory and Application*, ed. U. Landman (Plenum Press, New York, 1977), p. 441.
46. H. A. Bethe and E. Teller, Deviations from thermal equilibrium in shock waves, Report No. X-117, Ballistic Research Laboratory, Maryland, USA (1941).
47. L. Landau and E. Teller, *Phys. Z. Sowjetunion* **10**, 34 (1936).
48. V. M. Kenkre and R. S. Knox, *Phys. Rev. B* **9**, 5279 (1974).
49. V. M. Kenkre, *Phys. Rev. B* **11**, 3406 (1975).
50. M. Tiwari and V. M. Kenkre, *Eur. Phys. J. B* **87**, 1 (2014).
51. G. H. Wannier, *Rev. Mod. Phys.* **34**, 645 (1962).
52. J. B. Krieger and G. J. Iafrate, *Phys. Rev. B* **33**, 5494 (1986).
53. C. A. Moyer, *J. Phys. C* **6**, 1461 (1973).
54. D. Emin and C. F. Hart, *Phys. Rev. B* **36**, 2530 (1987).
55. P. R. Rider, *Ann. Inst. Stat. Math.* **9**, 215 (1957).
56. H. C. Wolf, Energy transfer in organic molecular crystals: A survey of experiments, in

Advances in Atomic and Molecular Physics, Vol. 3, eds. D. R. Bates and I. Eastermann (Academic Press, New York, 1967), pp. 119–142.
57. R. C. Powell and Z. G. Soos, *J. Lumin.* **11**, 1 (1975).
58. M. Abramowitz and I. E. Stegun, *Handbook of Mathematical Functions* (Dover, Toronto, 1970).
59. V. M. Kenkre and P. Reineker, *Exciton Dynamics in Molecular Crystals and Aggregates*, ed. G. Hoehler, Springer Tracts in Modern Physics, Vol. 94 (Springer, Berlin, 1982).
60. T. Förster, *Ann. Phys.* **2**, 55 (1948).
61. D. P. Visco, Jr. and S. Sen, *Phys. Rev. E* **57**, 225 (1998); **58**, 1419 (1998).
62. A. A. Ierides and V. M. Kenkre, Analysis of Inverted Temperature Dependence of Vibrational Relaxation Rates in Molecules Embedded in a Bath, University of New Mexico, preprint (2017).